Journal of Theoretical Biology 289 (2011) 173–180

Contents lists available at SciVerse ScienceDirect

Journal of Theoretical Biology

journal homepage: www.elsevier.com/locate/yjtbi

On the dynamic behaviour of the "click" mechanism in dipteran flight

Bin Tang [a,*], M.J. Brennan [b]

[a] Institute of Internal Combustion Engine, Dalian University of Technology, Dalian 116023, China
[b] Departamento de Engenharia Mecanica, Faculdade de Engenharia de Ilha Solteira (FEIS-Unesp), 15385-000, SP, Brasil

ARTICLE INFO

Article history:
Received 15 July 2011
Received in revised form
27 August 2011
Accepted 29 August 2011
Available online 1 September 2011

Keywords:
Insect flight motor
Mathematical model
Damping
Energy ratio
Bifurcation

ABSTRACT

In this paper, the dynamic behaviour of the "click" mechanism is analysed. A more accurate model is used than in the past, in which the limits of movement due to the geometry of the flight mechanism are imposed. Moreover, the effects of different damping models are investigated. In previous work, the damping model was assumed to be of the linear viscous type for simplicity, but it is likely that the damping due to drag forces is nonlinear. Accordingly, a model of damping in which the damping force is proportional to the square of the velocity is used, and the results are compared with the simpler model of linear viscous damping. Because of the complexity of the model an analytical approach is not possible so the problem has been cast in terms of non-dimensional variables and solved numerically. The peak kinetic energy of the wing root per energy input in one cycle is chosen to study the effectiveness of the "click" mechanism compared with a linear resonant mechanism. It is shown that, the "click" mechanism has distinct advantages when it is driven below its resonant frequency. When the damping is quadratic, there are some further advantages compared to when the damping is linear and viscous, provided that the amplitude of the excitation force is large enough to avoid the erratic behaviour of the mechanism that occurs for small forces.

1. Introduction

The flight mechanism of diptera has been studied for many years, and various mechanical models for this mechanism have been postulated. One such model, accepted by some in the community as being representative of the actual mechanism, involves the "click" mechanism (Boettiger and Furshpan, 1952; Pringle, 1957). Several papers on this topic have been written (for example, Thomson and Thompson, 1977; Miyan and Ewing, 1985, 1988; Bennet-Clark, 1986; Ennos, 1987; Pfau, 1987; Gronenberg, 1996; Brennan et al., 2003). Fig. 1 shows the flight mechanism described by Thompson and Thompson (1977). Brennan et al. (2003) proposed a simple mechanical model of this "click" mechanism, which is shown in Fig. 2a. Referring to this figure, the driving force from the scutellar lever is applied at C. The notum and pleural apophysis are modelled as two cantilever beams BE and DF, respectively. Rigid link ABC and CD, which represent the wing and parascutum, respectively, are pivoted at points B, C and D. The hinge at B represents the wing process. The hinge at C corresponds to the first axillary sclerite. Following analysis of the dynamics of this model they concluded that the "click" mechanism, which is inherently nonlinear, has advantages over a linear resonant mechanism provided that it is operated at a frequency much lower than the resonance frequency, which would be the case for very small flies. In that paper two main assumptions were made. The first was that the energy loss mechanism due to lift and drag forces on the wing could be represented by a linear viscous damper, and second was that the equation of motion of the mechanical model could be simplified to the Duffing equation (Kovacic and Brennan, 2011).

Recently, Cheng et al. (2010) analysed the influence of body rotation on the aerodynamic force and torque production during fast turning manueuvers in the fruit fly *Drosophila*. The damping coefficients and time constants were estimated based on both simulations and experimental results to obtain the effects of passive aerodynamic damping in turning flight. In the flight mechanism of diptera, the damping force due to the aerodynamics is strongly influenced by the Reynolds number. When a body passes through a fluid at high Reynolds numbers, the flow separates and the drag force is nearly proportional to the square of the velocity and can be treated as a quadratic damping force. When the Reynolds number is small the advective inertial forces are small and the damping force can be assumed to be proportional to the velocity (Nayfeh and Mook, 1995). Because of the small size and relatively low flight velocity, the Reynolds number for an insect is smaller than a bird and common air vehicles. For the smallest insects, which weigh about 20–30 μg, the Reynolds number is about 10, while the Reynolds number for large insects, which weigh about 2–3 g is around 5000–10000 (Ellington, 1999; Meuller and DeLaurier, 2003).

* Corresponding author.
E-mail address: btang@dlut.edu.cn (B. Tang).

0022-5193/$ - see front matter © 2011 Elsevier Ltd. All rights reserved.
doi:10.1016/j.jtbi.2011.08.039

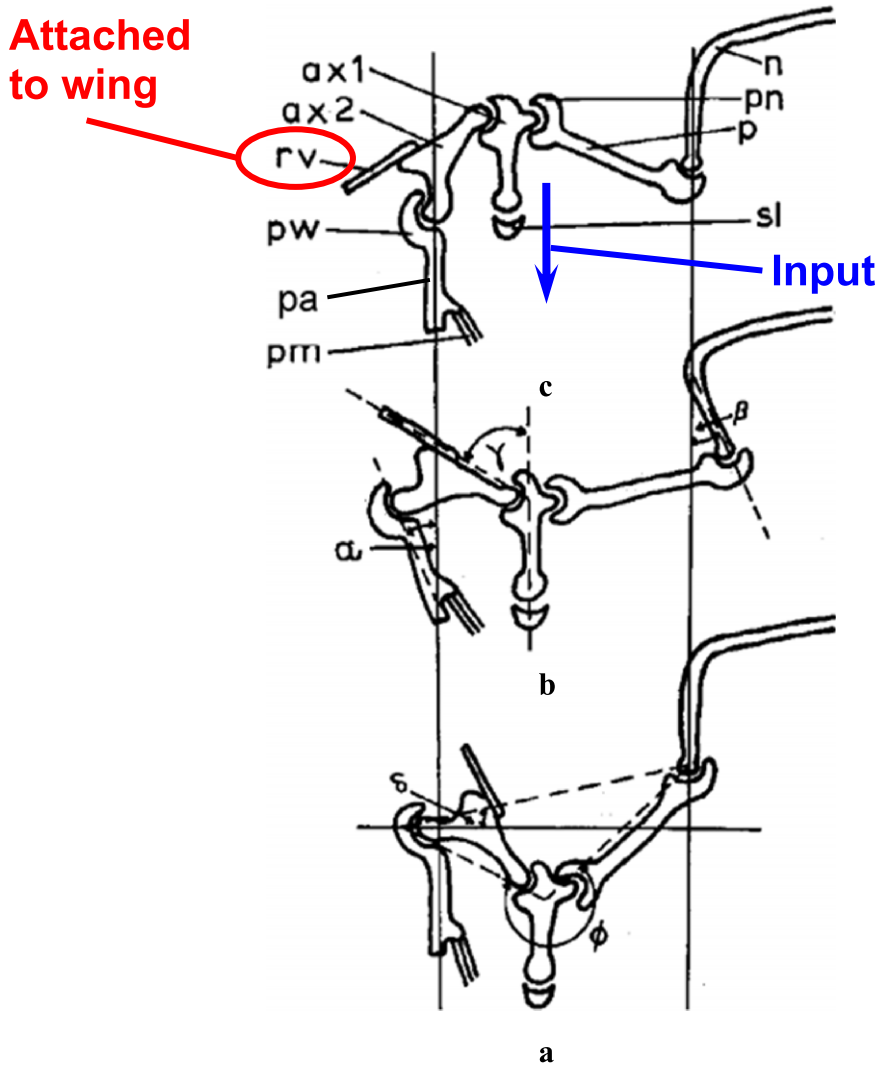

Fig. 1. (a–c) Diagram showing the flight motor of an insect and three successive positions of the wing articulation during the course of a beat, from the up position (a) to the down position (c); ax1, ax2—axillary sclerites 1 and 2; n—notum; p—parascutum; pm—pleurosternal muscle; pn—anterior notal process; pw—wing process; rv—base of radial vein; sl—section through scutellar lever (after Thomson and Thompson, 1977); pa—pleural apophysis (shown in Pringle, 1957).

Thus, for small diptera, the damping force may lie somewhere between linear and quadratic forms.

The aim of this paper is to further investigate the dynamic model of the "click" mechanism investigated by Brennan et al. (2003). The assumptions they made (given above) are revisited and a more accurate description of the dynamic behaviour of the model is sought. The relative influence of linear and quadratic damping forces is investigated and a numerical method is used to investigate the dynamic behaviour.

2. Dynamical model

The perturbed model of the flight mechanism of Fig. 2a is shown in Fig. 2b. The displacement of the mass y is the instantaneous elevation of C from BD and x is the lateral bending of the cantilevers. This model has three static equilibrium positions as shown in Fig. 2c. When the cantilevers have no deformation, there are two stable static equilibrium positions corresponding to the dotted and the dashed-dotted lines. When C lies on the line BD, such that the wing is in the horizontal position, the system is in a static unstable equilibrium position; any perturbation results in the system to move to one of the stable equilibrium positions. The mass C can move in positive and negative directions along the y axis. The potential energy of the system shown in Fig. 2b is given by

$$U = k\left(-b+\sqrt{l^2-y^2}\right)^2 \tag{1}$$

where k is the bending stiffness of each of the two vertical uniform cantilever beams, $2b$ is the distance between the two cantilever beams and l is the length of BC or CD. The restoring force can be obtained by the taking the derivative of the potential energy to give $2k(-1+b/\sqrt{l^2-y^2})y$. When this is combined with the mass m, and a sinusoidal exciting force of amplitude P and frequency ω is applied, the resulting equation of motion is given by

$$m\ddot{y}+2k\left(-1+\frac{b}{\sqrt{l^2-y^2}}\right)y = P\cos\omega t \tag{2}$$

Assuming linear viscous damping with damping coefficient c_1 a non-dimensional equation of motion can be written as

$$u''+\gamma_1 u'-\alpha u+\alpha\beta\frac{u}{\sqrt{1-u^2}} = F\cos\Omega\tau \tag{3}$$

where $u=y/l$, $\gamma_1=c_1/m\omega_0$, $\omega_0^2=2k(1/\beta^2-1)/m$, $\beta=b/l$, $F=P/ml\omega_0^2$, $\tau=\omega_0 t$, $\Omega=\omega/\omega_0$, $\alpha=\beta^2/(1-\beta^2)$ and $(\bullet)'$ denotes differentiation

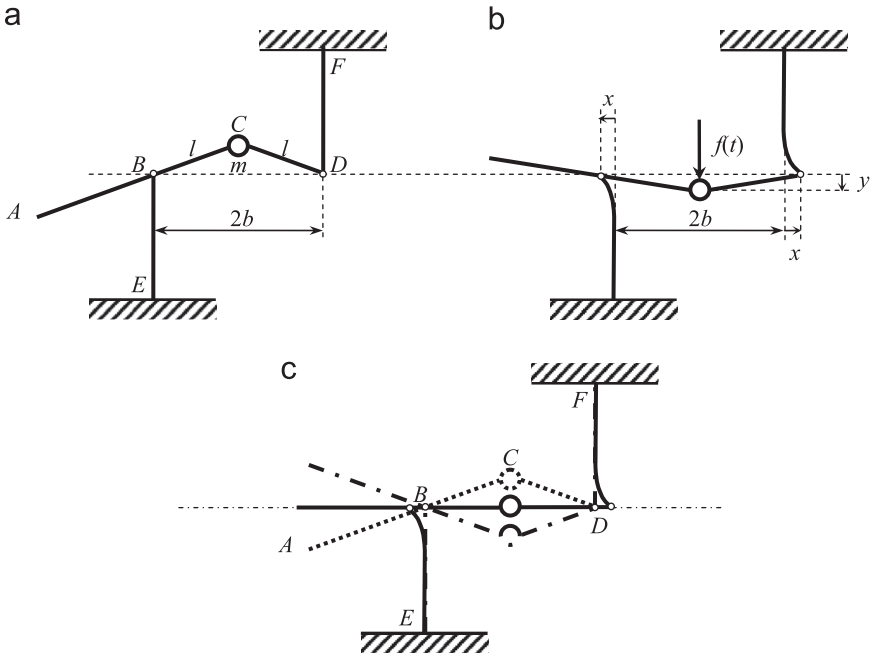

Fig. 2. Simplified mechanical model of the fight motor with the click mechanism: (a) simplified model, (b) model showing the coordinates, (c) model at its equilibrium positions—two stable (dashed and dashed dotted lines), and one unstable (solid line).

with respect to non-dimensional time τ. Note that ω_0 is the natural frequency for small oscillations when the system is at either of its static equilibrium positions. If quadratic damping is assumed with damping coefficient c_2, the corresponding non-dimensional equation of motion is given by

$$u''+\gamma_2 u'|u'|-\alpha u+\alpha\beta\frac{u}{\sqrt{1-u^2}}=F\cos\Omega\tau \tag{4}$$

where $\gamma_2=c_2 l/m$.

3. Dynamic analysis and simulations

3.1. Introduction

It is can be seen from Eqs. (3) and (4) that there is a limitation of $|u|<1$ on the non-dimensional displacement of the click mechanism, because of the term $\sqrt{1-u^2}$, which is a consequence of the model geometry. This simply means that the vertical displacement y cannot exceed the length of the rigid link l. In the previous work by Brennan et al. (2003), Eq. (3) was approximated to $u''+\gamma_1 u'-\alpha(1-\beta)u+(\alpha\beta/2)u^3=0$, which is a form of the Duffing equation with a negative linear stiffness and a positive cubic nonlinear stiffness (Kovacic and Brennan, 2011). This was done to simplify the equation, but it means that the limitation of $|u|<1$ is removed (at least mathematically) and thus the dynamics of the actual model differs appreciably from the approximate model for large displacements. The approximation meant that analytical solution methods could then easily be applied to the problem. However in this paper, more accurate results are sought, so a numerical method is used to solve the actual equations of motion instead. To illustrate some basic differences between the actual model and the approximate one given by the Duffing equation, the non-dimensional restoring force, potential energy and stiffness are given in Fig. 3a, b and c, respectively. It can be seen that for values of $|y/l|$ less than about 0.4, the approximate model is a reasonable representation of the actual model, but for values greater than this, the discrepancy between the models increases. In Fig. 3b, the stable (a, c) and unstable (b) equilibrium positions are shown. It can be seen that they are slightly different for each system. The stiffness of the system at the stable equilibrium positions can be seen by following the vertical dashed lines down to Fig. 3c and are given by $2k(l^2/b^2-1)$ for the actual model and $4k(1-b/l)$ for the approximate model, with corresponding natural frequencies of $2k(l^2/b^2-1)/m$ and $4k(1-b/l)/m$. For a value of $b/l=0.9$, the natural frequency of the approximate system is only about 92% of the natural frequency of the actual model. For excursions of the mass of $|y/l|>0.4$ the stiffness of the systems becomes markedly different. In the actual model as $|y/l|\to 1$ the stiffness becomes infinite as it is assumed that the links are rigid. This will have a profound influence on the dynamic behaviour of the actual system compared to the approximate model for large displacements.

3.2. Choice of damping parameters

To compare the systems with linear and quadratic damping, suitable values of damping have to be chosen. This is considered in this section.

In Eq. (3) the linear damping factor is given by $\gamma_1=c_1/m\omega_0$ in which $\omega_0=\sqrt{2k(1/\beta^2-1)/m}$. This can be written as $\gamma_1=2\zeta_1/\sqrt{2(1/\beta^2-1)}$, where $\zeta_1=c_1/2\sqrt{mk}$, which is the conventional damping ratio of a linear single degree-of-freedom system. Because insect flight will induce a large damping force because of the lift and drag forces, and one of the findings of Brennan et al. (2003) was that the click mechanism is only advantageous if the damping is large, only a heavily damped case is considered here. Assuming a value of $\zeta_1=0.5$, as in Brennan et al. (2003), it is found that $\gamma_1\approx 1.46$.

To determine an appropriate value of γ_2, two dampers – the linear and the quadratic damper – are considered separately from the rest of the system. They are subjected to a harmonic force of frequency ω such that the amplitude of the relative displacement across the dampers is U. The energy dissipated by the linear damper in one cycle of vibration is then given by $E_1=\pi c_1\omega U^2$ and for the quadratic damper $E_2=8c_2\omega^2U^3/3$ (Ruzicka and Derby,

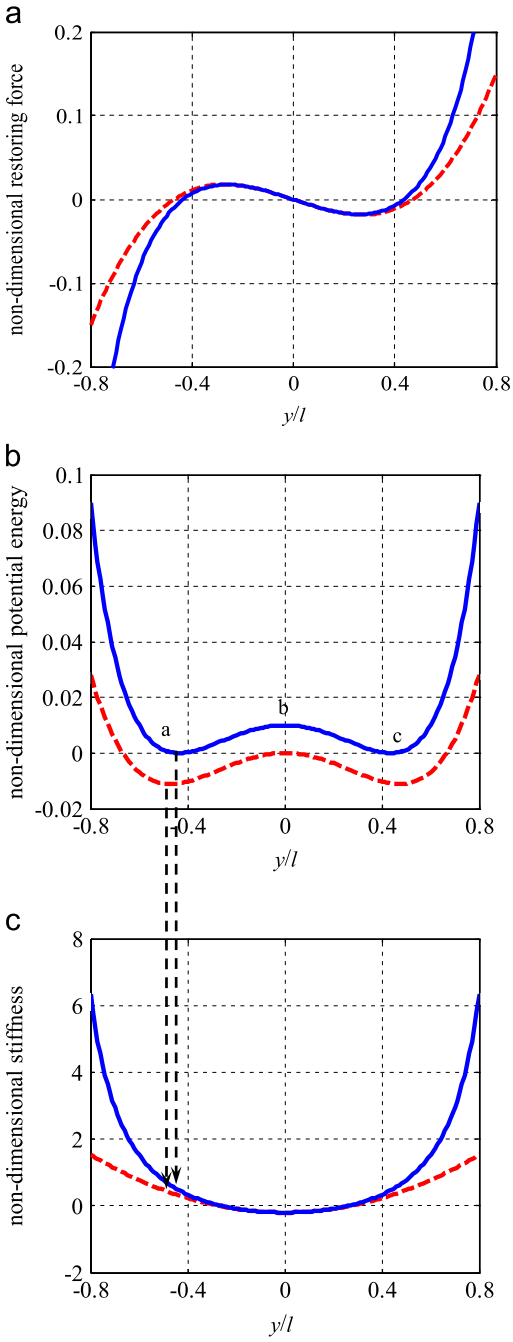

Fig. 3. Static characteristics of the "click" mechanism shown in Fig. 2, for a value of $\beta=0.9$. (a) Non-dimensional restoring force of the mechanism, (b) non-dimensional potential energy of the mechanism, (c) non-dimensional stiffness of the mechanism. Solid blue line, actual; dashed red line, approximation. (For interpretation of the references to colour in this figure legend, the reader is referred to the web version of this article.)

1971). If the energy dissipated by the dampers is set to be equal so that $E_1=E_2$ then $c_2=3\pi c_1/8\omega U$. This results in $\gamma_2=(3\pi/8\Omega U)\gamma_1$. If the frequency and amplitude are set such that $\Omega=1$ and $U=1$, then $\gamma_2\approx 1.72$.

3.3. Comparison of different mechanisms

In this section the nonlinear "click" mechanism systems with linear and quadratic damping are compared with the linear resonant system. To carry out this comparison, the time histories of the responses described by Eqs. (3) and (4) are determined using a time-domain integration method, which are then subsequently processed to determine the effectiveness of each system to see which one is most advantageous for small diptera.

The fourth-order Runge–Kutta method with a step-size control algorithm (Hairer et al., 1993) was used to obtain the numerical time domain response of the systems. For values of the geometrical parameter $\beta=0.9$ and non-dimensional force amplitude of 2.0, two excitation frequencies are considered, $\Omega=0.1$ and $\Omega=1.0$. The non-dimensional steady-state displacements of the two systems are shown in Fig. 4. It can be seen that the two systems have very different responses both when excited well below the resonance frequency and at the resonance frequency. In the non-resonant case, the time history response waveforms of the systems are not sinusoidal. Moreover, the higher the non-dimensional excitation force amplitude, the larger the high frequency components in the responses. The time history response curves excited at the resonance frequency are similar to a distorted triangular wave. As the excitation force amplitude increases, in this case the time history response curves distort even more. It should also be noted that when $\Omega=0.1$, there are more high frequency oscillations in the system with quadratic damping force.

As discussed by Brennan et al. (2003), when the excitation frequency is much less than the resonance frequency, for example when $\Omega=0.1$, the heavily damped "click" mechanism can give some advantages for diptera flight. The increased gradient of the displacement during the down-stroke as seen in Fig. 4a and b means that the wings can experience a larger velocity for a given maximum displacement. This can give greater lift than would be obtainable with a linear resonant system.

When both the linear and quadratic damping ratios are reduced to a small value, for example, one-tenth of the damping ratios used above, the quadratic damping force becomes smaller than the linear damping force. Consequently, the high frequency oscillations will be very large for the system with quadratic damping at non-resonant conditions. At resonant conditions, the displacement y reaches a value of l, the maximum value that it can attain because of the geometry of the system. The time history response curves for the systems with small damping are not given here, however, because it is not believed to be relevant to small diptera.

To compare the effectiveness of the "click" mechanism for the two damping models, the approach taken by Ellington (1999) and Brennan et al. (2003) is followed. The output of the system is considered to be the peak velocity of the wing, characterised here by the peak kinetic energy of the mass, and the input to the system is the work input. The ratio of these quantities is calculated over one period of excitation, and the system with the highest ratio is deemed to have a better performance.

The non-dimensional peak kinetic energy of the system in the steady-state is given by $(u'_{peak})^2/2$. The ratio of non-dimensional peak kinetic energy to work input over one cycle (henceforth called the energy ratio for brevity) is thus given by

$$\hat{E}=\frac{\text{Peak kinetic energy}}{\text{Work input over one cycle}}=\frac{(u'_{peak})^2/2}{\Omega\int_0^{2\pi/\Omega}F\cos\Omega\tau u'\,d\tau} \tag{5}$$

Eq. (5) is evaluated numerically from the time series calculated using the Runge–Kutta method after 300 cycles of excitation (to ensure a steady-state response). The results for linear damping are shown in Fig. 5a. From this figure, it can be seen that the "click" mechanism has a distinct advantage in the non-resonant case, and the difference between the resonant "click" mechanism and linear system is negligible. The peak kinetic energy of the linear system is given by $1/(4\pi\zeta_1)$ (Brennan et al., 2003). According to the discussion in Section 3.2, ζ_1 is assumed to be 0.5 for the linear system. It can be seen that when the amplitude of the non-dimensional excitation force is greater than about 0.1 the energy

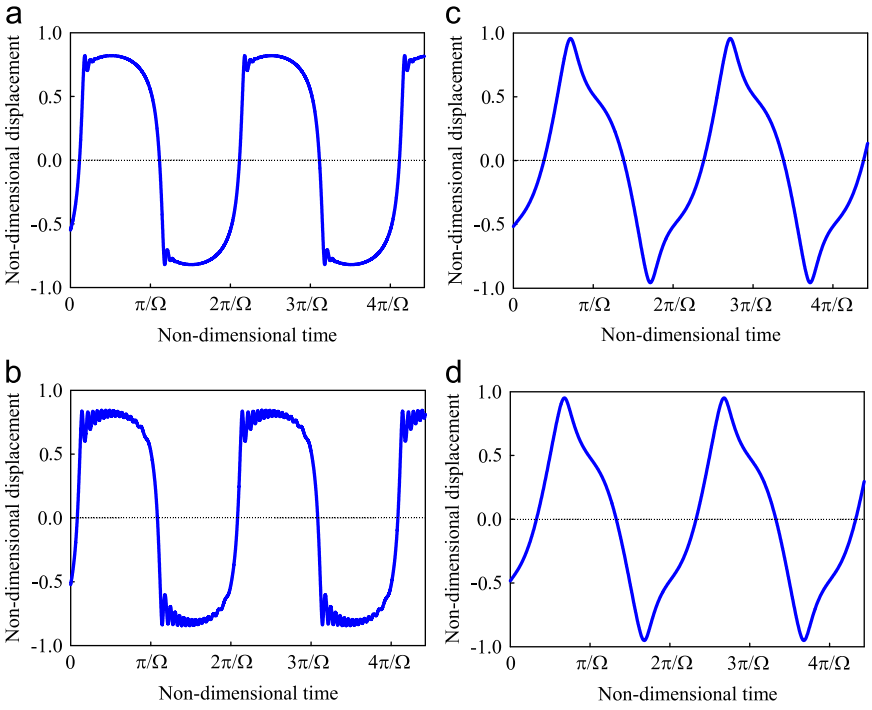

Fig. 4. Displacement response of the system with "click" mechanism with linear and quadratic damping, when $\beta=0.9$ and $F=2.0$. The response were calculated using the Runge–Kutta method with a step size control algorithm, (a) $\Omega=0.1$, $\gamma_1=1.46$ (low frequency, linear damping); (b) $\Omega=0.1$, $\gamma_2=1.72$ (low frequency, quadratic damping); (c) $\Omega=1.0$, $\gamma_1=1.46$ (resonance frequency, linear damping) and (d) $\Omega=1.0$, $\gamma_2=1.72$ (resonance frequency, quadratic damping).

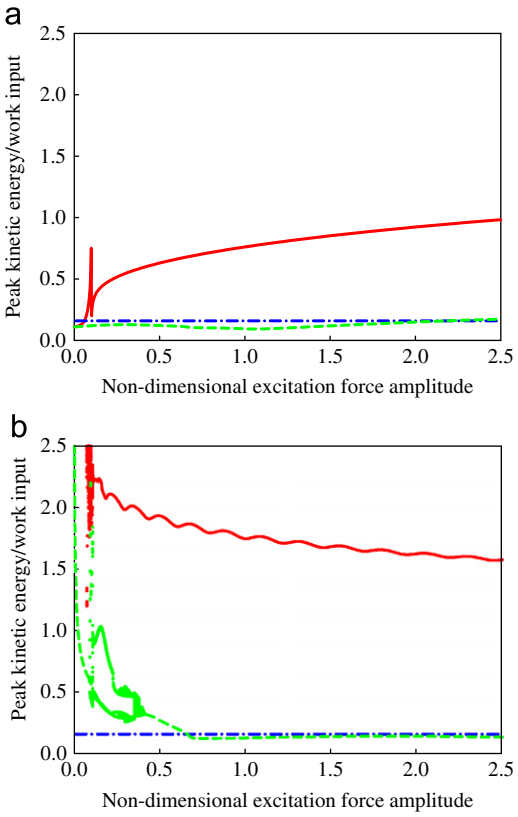

Fig. 5. Ratio of peak kinetic energy of the "click" mechanism to the work input in one cycle as a function of non-dimensional excitation force amplitude with $\beta=0.9$ and (a) linear damping $\gamma_1=1.46$, (b) quadratic damping $\gamma_2=1.72$. Solid red line, when $\Omega=0.1$; dashed green line, $\Omega=1.0$, dashed-dotted blue line, linear system with $\zeta_1=0.5$. (For interpretation of the references to colour in this figure legend, the reader is referred to the web version of this article.)

ratio for the non-resonant case increases monotonically with force amplitude and is larger than that for the resonant systems. It increases until the non-dimensional displacement reaches a value of 1, which corresponds to non-dimensional force amplitudes of about 3.1. The reason for the small peak for the non-resonant condition ($\Omega=0.1$) is given below.

In Appendix A, it is shown that when the non-dimensional force is about 0.1, the phase between the force and the velocity changes rapidly for a very small range of force amplitude. It is this rapid change in phase between the force and velocity that results in the rapid change in energy supplied to the system, which is reflected in the erratic behaviour of the solid red line in Fig. 5a when the non-dimensional force amplitude is about 0.1. Above this value of force the ratio given in Eq. (5), which is taken as a measure of the efficiency of the system, gradually increases, as the phase between the force and the velocity diverges tending to a value close to 90° as the excitation force becomes increasingly large. Thus the reason why the "click" mechanism is increasingly more effective as the excitation force increases is because this has the effect of changing the phase between the response and the excitation force, meaning that less energy is input to the system. Moreover, for a given maximum amplitude of displacement and excitation frequency, the "click" mechanism facilitates the generation of a higher peak velocity.

The corresponding results for the "click" mechanism with quadratic damping ratio are shown in Fig. 5b. When the excitation force amplitude is small, the nonlinear system responses are very erratic. With an increase in the amplitude of the excitation force, the system responses become more regular, and the energy ratio begins to decrease. It can be seen that provided the non-dimensional amplitude of the excitation force is above about 0.1, the "click" mechanism with quadratic damping outperforms the system with linear damping under non-resonant condition. It is interesting to note that the energy ratio curve for $\Omega=0.1$ decreases with the increasing excitation force amplitude, which

is the opposite trend to the system with the linear damper. In an attempt to understand this result, a SDOF of system with a linear spring and with quadratic damping is discussed in Appendix B. It can be seen that the reason for the reduction in the energy ratio as the amplitude of the excitation force increases is as follows. Although the velocity of the system increases as the force increases, the power input also increases as force increases, but at a greater rate than the velocity increase. The net result is that the energy ratio decreases as the force increases, which is *not* the case when the damping is linear.

To further investigate the dynamic characteristics of the system and erratic behaviour of the energy ratio for small excitation force amplitudes, bifurcation diagrams for the "click" mechanism with both linear and quadratic damping force are presented in Fig. 6. The initial conditions were set to $u(0)=0$, $u'(0)=0$, and the solutions were calculated for 300 limit cycles. The transient parts are ignored and only the last 50 peak displacement values are plotted.

For the heavily linear damped "click" mechanism as shown in Fig. 6a and b, the system response is periodic. The transition point 1 in these two figures marks the change in the equilibrium position for the oscillations; for small force amplitudes the system oscillates in one of the wells shown in Fig. 3b, about either positions a or c, and for larger forces the system undergoes larger oscillations about the unstable equilibrium position, b (so-called two-well oscillations). The time history response for the system excited at the resonance frequency is almost sinusoidal when the amplitude of the excitation force is between the transition points 1 and 2. The nonlinear influence on the displacement in this region is not very strong. However, after point 2, the response curve distorts becoming similar to a triangular waveform due to the influence of the high nonlinear spring force. These transition points are also evident on the energy ratio curves in Fig. 5a.

The bifurcation diagrams for the system with quadratic damping $\gamma_2=1.72$ are plotted in Fig. 6c and d. When $\Omega=0.1$, as in Fig. 6c the system response becomes very erratic for an excitation force amplitude of around 0.1. For higher amplitudes of excitation force, the system response becomes periodic. It can be seen in the inset of Fig. 6c, that the displacement increases, but with a slight ripple as the amplitude of the excitation force increases, then becomes smoother.

In Fig. 6c and d it can be seen that the range of force amplitudes when the response of the system is erratic is larger when it is excited at its resonance frequency than when it is excited at a much lower frequency. The system response becomes more regular when the amplitude of the excitation force amplitude is greater than about 0.5. The transition point 2 can also be seen in Fig. 6d, which indicates the point at which the displacement changes from a sinusoidal waveform due to the influence of the nonlinear characteristics of the system.

4. Conclusions

A model of the "click" mechanism in the flight motor small diptera has been investigated to determine whether this mechanism has advantages compared to a linear resonant system. Unlike in previous work, the analysis has been carried out using the original equation of motion, rather than an approximate one based on the Duffing equation. This equation has the limitation of the maximum response amplitude because of the physical structure of the mechanism. Because the damping in the system may be proportional to the square of the velocity of the wing

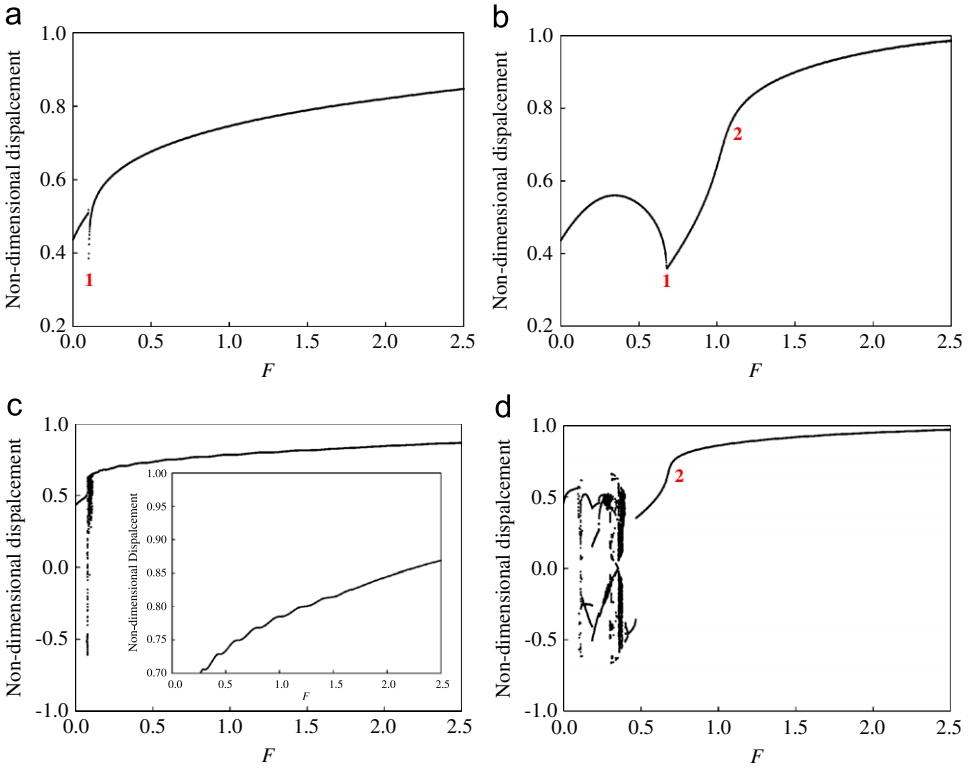

Fig. 6. Bifurcation diagram of the "click" mechanism with linear and quadratic damping force, when $\beta=0.9$, $f(\tau)=F\sin\Omega\tau$, $\Delta F=0.001$, $\Delta\tau=0.01$, $n=300$(300 cycles), $u_0=0.0$, $u_0'=0.0$. (a) $\Omega=0.1$, linear damping $\gamma_1=1.46$; (b) $\Omega=1.0$, linear damping $\gamma_1=1.46$; (c) $\Omega=0.1$, quadratic damping $\gamma_2=1.72$ and (d) $\Omega=1.0$, quadratic damping $\gamma_2=1.72$. Point 1 indicates when the system changes from one-well motion to two-well motion; Point 2 indicates when the amplitude of the excitation force results in strong nonlinear effects in which the response consists of many harmonics of the excitation frequency.

rather than the velocity of the wing, the effects of linear and quadratic damping on the dynamic behaviour of the "click" mechanism have been investigated.

From the time history response, the ratio of non-dimensional peak kinetic energy to work input over one period of excitation (energy ratio) and the bifurcation diagrams have been obtained for each system. It has been shown that when the "click" mechanism with linear damping is excited well below its resonance frequency, the energy ratio (and hence the wing velocity) increases with an increase in the amplitude of the excitation force. It has also been shown that this system outperforms both the same system excited at the resonance frequency and a linear resonant system. Moreover it has been shown that the non-resonant system with quadratic damping outperforms the same system with linear damping. This suggests that the "click" mechanism has further advantages for larger diptera when the Reynolds number is large, such that the damping mechanism on the structure due to air is quadratic rather than linear.

Acknowledgements

The first author wishes to acknowledge the financial support from the China Scholarship Council (Grant 2009821053), which enabled him to complete the paper at the Institute of Sound and Vibration Research, University of Southampton, UK, and Doctoral Scientific Research Starting Foundation of Liaoning Province of China (Grant 20091014).

Appendix A. Phase differences between the force and the responses in system with the "click" mechanism

To gain insight into the shape of the curve in Fig. 5, the relationship between the phase differences between the excitation force and the fundamental Fourier components of the displacement and velocity responses at the excitation frequency is investigated for $\Omega=0.1$. They are plotted as a function of the non-dimensional force amplitude in Fig. A1. The phase differences are determined using the fast Fourier transform of the time histories of force, displacement and velocities, with corrections being made for the window function used (Xie and Ding, 1996).

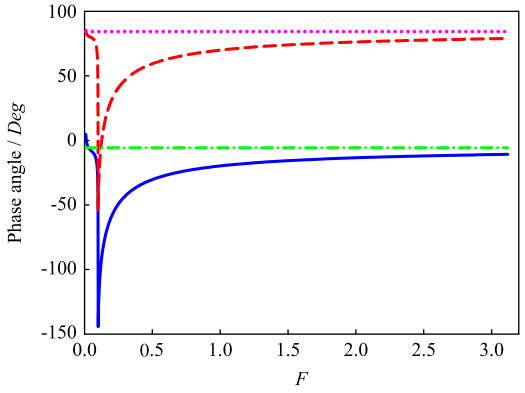

Fig. A1. Phase differences between the force and the primary harmonic terms of displacement and velocity response of "click" mechanism with linear damping when $\Omega=0.1$, $\beta=0.9$ and $\gamma_1=1.46$. Solid blue line, phase differences between the force and the primary harmonic terms of displacement response; dashed red line, phase differences between the force and the primary harmonic terms of velocity response; dash-dotted green line, phase differences between the force and the displacement response for the linear system when $\Omega=0.1$, $\zeta_1=0.5$; dotted pink line, phase differences between the force and the velocity response for the linear system when $\Omega=0.1$, $\zeta_1=0.5$. (For interpretation of the references to colour in this figure legend, the reader is referred to the web version of this article.)

Note that there is 90° of phase difference between the velocity and the displacement for all values of force. Note also that when the non-dimensional force is about 0.1 the phase changes rapidly for a small change in excitation force, and there are two amplitudes of excitation force when the force and the velocity are in phase. In between these values it dips to about $-50°$. When the velocity and the force are in-phase the power supplied to the system is the maximum (Den Hartog, 1947). As the force increases above about 0.1, the phases gradually change so that eventually the velocity leads the force by about 84.32° and the displacement lags the force by 5.68° These values correspond to the linear system with $\zeta_1=0.5$. Thus, for high values of excitation force, the force and the velocity are almost in quadrature and hence there is very little energy input to the system when the non-dimensional frequency is 0.1.

Appendix B. Response of a SDOF system with a linear spring and quadratic damping

To help understand why the energy ratio of the system with quadratic damping decreases as the amplitude of the excitation force increases, a similar system, but with a linear spring, is analysed in this appendix. The reason for this is that a simple closed-form solution for the energy ratio can be determined using the harmonic balance method.

The equation of motion for a single degree-of-freedom system with linear spring and quadratic damper can be written as

$$m\ddot{y}+c_2\dot{y}|\dot{y}|+ky=P\cos\omega t \tag{B.1}$$

When the non-dimensional parameters $u=y/l$, $\gamma_2=c_2l/m$, $\omega_0^2=k/m$, $F=P/ml\omega_0^2$, $\tau=\omega_0 t$, $\Omega=\omega/\omega_0$ are introduced, Eq. (B.1) becomes

$$u''+\gamma_2u'|u'|+u=F\cos\Omega\tau \tag{B.2}$$

where the primes denote the derivatives with respect to non-dimensional time τ. The initial conditions considered are

$$u(0)=0,u'(0)=0 \tag{B.3}$$

The solution of Eq. (B.2) is assumed to be harmonic with the form $u=U\cos(\Omega\tau+\phi)$. The stiffness and damping forces can be can be approximated by Fourier expansion up to first order as (Ravindra and Mallik, 1994)

$$\gamma_2u'|u'|+u=U\cos(\Omega\tau+\phi)-\frac{8\gamma_2U^2\Omega^2}{3\pi}\sin(\Omega\tau+\phi) \tag{B.4}$$

Thus Eq. (B.2) becomes

$$-\Omega^2U\cos(\Omega\tau+\phi)+U\cos(\Omega\tau+\phi)-\frac{8\gamma_2U^2\Omega^2}{3\pi}\sin(\Omega\tau+\phi)=F\cos\Omega\tau \tag{B.5}$$

Equating coefficients of the same harmonics results in

$$\frac{64}{9\pi^2}\gamma_2^2\Omega^4U^4+\Omega^4U^2-2\Omega^2U^2+U^2=F^2 \tag{B.6}$$

$$\phi=\arctan\frac{8\gamma_2\Omega^2U}{3\pi(\Omega^2-1)} \tag{B.7}$$

when $\Omega=1.0$, $U=\sqrt{3\pi F/8\gamma_2}$ and $\phi=-\pi/2$. When the system is excited by $F\cos\tau$, the displacement response is $u=\sqrt{3\pi F/8\gamma_2}\sin\tau$, and the velocity response is $u'=\sqrt{3\pi F/8\gamma_2}\cos\tau$. Substituting the displacement and velocity responses in Eq. (5) gives $\hat{E}=\sqrt{3/32\pi\gamma_2F}$, which is the closed-form energy ratio for the linear spring system with a quadratic damper. Thus, although the peak kinetic energy is proportional to F, the work input over

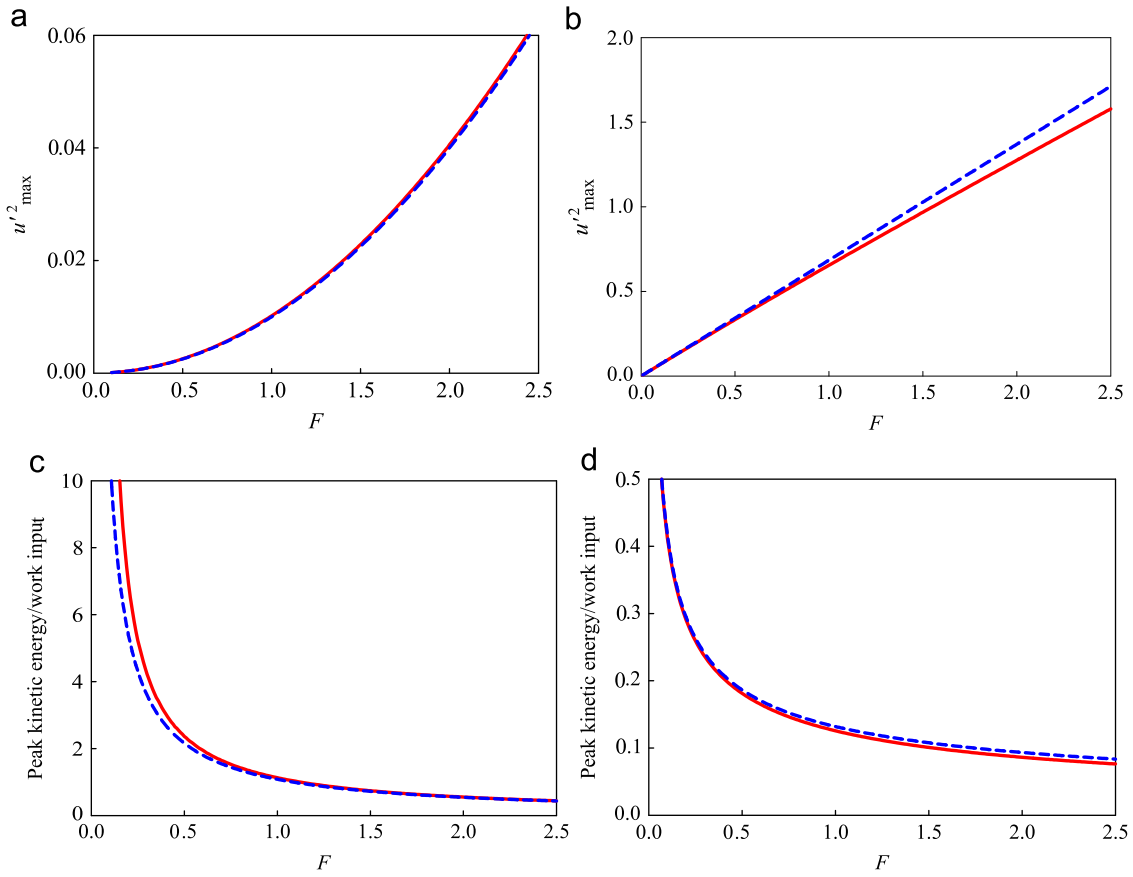

Fig. B1. (a and b) Maximum of the squared velocity and (c and d) the ratio of peak kinetic energy to work input of the linear spring system with quadratic damper when $\gamma_2=1.72$, (a), (c) $\Omega=0.1$; (b), (d) $\Omega=1.0$. Solid red line, numerical results; dashed blue line, closed-form solutions. (For interpretation of the references to colour in this figure legend, the reader is referred to the web version of this article.)

one cycle is proportional to $F^{3/2}$ so the energy ratio at the resonance frequency is proportional to $F^{-1/2}$.

When $\Omega \ll 1.0$, $U \approx F$ and the system is excited by $F\cos\tau$, the displacement response is $u \approx F\cos(\Omega\tau+\phi)$, and the velocity response $u' \approx -\Omega F\sin(\Omega\tau+\phi)$. Substituting the displacement and velocity responses in Eq. (5) gives $\hat{E}=3(1-\Omega^2)/16\gamma_2\Omega F$. Thus, in this case the peak kinetic energy is proportional to F^2. The work input over one cycle is proportional to F^3 so the energy ratio at the resonance frequency is proportional to F^{-1}.

To illustrate these cases, the closed-form and numerical results for the linear spring system with quadratic damper excited at $\Omega=0.1$ and $\Omega=1.0$ are given in Fig. B1. It can be seen that the closed-form results compare reasonably well with the numerical results. The energy ratios decrease when the excitation force amplitude increases in the manner discussed above.

References

Bennet-Clark, H.C., 1986. The flight of the dipteran fly. Nature 321, 468–469.

Boettiger, E.G., Furshpan, E., 1952. The mechanics of flight movement in diptera. Biol. Bull. 102, 200–211.

Brennan, M.J., Elliott, S.J., Bonello, P., Vincent, J.F.V., 2003. The "click" mechanism in diperan flight: if it exists, then what effect does it have? J. Theor. Biol. 224, 205–213.

Cheng, B., Fry, S.N., Huang, Q., Deng, X., 2010. Aerodynamic damping during rapid flight maneuvers in the fruit fly *Drosophila*. J. Exp. Biol. 213, 602–612.

Ellington, C.P., 1999. The novel aerodynamics of insect flight: applications to micro-air vehicles. J. Exp. Biol. 202, 3439–3448.

Ennos, A.R., 1987. A comparative study of the flight mechanism of diptera. J. Exp. Biol. 127, 355–372.

Gronenberg, W., 1996. Fast actions in small animals: springs and click mechanisms. J. Comp. Physiol. A 178, 727–734.

Hairer, E., Nørsett, S.P., Wanner, G., 1993. Solving Ordinary Differential Equations I: Nonstiff Problems, second ed. Springer-Verlag, Berlin.

Kovacic, I., Brennan, M.J., 2011. The Duffing Equation: Nonlinear Oscillators and their Behaviour. Wiley, Chichester.

Mueller, T.J., DeLaurier, J.D., 2003. Aerodynamics of small vehicles. Annu. Rev. Fluid Mech. 35, 89–111.

Miyan, J.A., Ewing, A.W., 1985. Is the 'click' mechanism of dipteran flight an artefact of CCl_4 anaesthesia? J. Exp. Biol. 116, 313–322.

Miyan, J.A., Ewing, A.W., 1988. Further observations on dipteran flight: details of the mechanism. J. Exp. Biol. 136, 229–241.

Nayfeh, A.H., Mook, D.T., 1995. Nonlinear Oscillations. John Wiley & Sons, New York.

Pfau, H.K., 1987. Critical comments on a 'novel mechanical model of dipteran flight' (MIYAN & EWING, 1985). J. Exp. Biol. 128, 463–468.

Pringle, J.W.S., 1957. Insect Flight. Cambridge University Press, Cambridge.

Ravindra, B., Mallik, A.K., 1994. Performance of non-linear vibration isolators under harmonic excitation. J. Sound Vib. 170, 325–337.

Ruzicka, J.E., Derby, T.F., 1971. Influence of Damping in Vibration Isolation. The Shock and Vibration Information Center, Washington.

Thomson, A.J., Thompson, W.A., 1977. Dynamics of a bistable system: the click mechanism in dipteran flight. Acta Biotheor. 26, 19–29.

Xie, M., Ding, K., 1996. Corrections for frequency, amplitude and phase in a fast Fourier transform of a harmonic signal. Mech. Syst. Signal Process. 10, 211–221.

Den Hartog, J.P., 1947. Mechanical Vibrations, third ed. McGraw-Hill, New York.